

Chemical Synthesis, 3D Structure, and ASIC Binding Site of the Toxin Mambalgin-2**

Christina I. Schroeder, Lachlan D. Rash,* Xavier Vila-Farrés, K. Johan Rosengren, Mehdi Mobli, Glenn F. King, Paul F. Alewood, David J. Craik, and Thomas Durek*

Abstract: Mambalgins are a novel class of snake venom components that exert potent analgesic effects mediated through the inhibition of acid-sensing ion channels (ASICs). The 57-residue polypeptide mambalgin-2 (Ma-2) was synthesized by using a combination of solid-phase peptide synthesis and native chemical ligation. The structure of the synthetic toxin, determined using homonuclear NMR, revealed an unusual three-finger toxin fold reminiscent of functionally unrelated snake toxins. Electrophysiological analysis of Ma-2 on wild-type and mutant ASIC1a receptors allowed us to identify α -helix 5, which borders on the functionally critical acidic pocket of the channel, as a major part of the Ma-2 binding site. This region is also crucial for the interaction of ASIC1a with the spider toxin PcTx1, thus suggesting that the binding sites for these toxins substantially overlap. This work lays the foundation for structure–activity relationship (SAR) studies and further development of this promising analgesic peptide.

Animal venoms are essentially large combinatorial libraries of bioactive molecules, which hold great promise as diagnostic tools and for the treatment of human diseases.^[1] The vast majority of these compounds are disulfide-rich polypeptides of 10–80 amino acid residues that adopt highly ordered 3D structures and potentially modulate the activity of specific classes of membrane proteins such as ion channels, receptors, and transporters. Mambalgins are a recently discovered class

of peptides isolated from the venom of black mamba snakes. They are comprised of 57 residues that form a structure cross-braced by four disulfide bridges.^[2] The mambalgins are potent blockers of acid-sensing ion channels (ASICs) and in animal models, they show potent central and peripheral analgesic effects without the side effects associated with traditional opioid drugs.^[2a] In addition to a role in pain perception, this family of proton-gated cation channels has been implicated in neurodegeneration, fear- and anxiety-related behavior, brain-tumor growth, and sensory transduction.^[3]

Based on the number and location of the cysteine residues and the length of the inter-cysteine sequences (loops), the mambalgins were proposed to adopt a three-finger toxin (TFT) fold reminiscent of the functionally unrelated short-chain neurotoxins commonly found in snake venom.^[4] However, the disulfide connectivity has not been determined experimentally, the inter-cysteine loops show very limited similarity to known TFTs, and the mambalgins possess activity not previously observed for TFTs, thereby raising the possibility that the mambalgins have a unique 3D fold (see the Supporting Information). To address this possibility and to establish a robust platform for detailed structure–activity–relationship (SAR) studies, we report herein the first efficient chemical synthesis and 3D structure determination of a member of the mambalgin family (Ma-2).

We set out to chemically synthesize the entire 57-residue Ma-2 by step-wise Fmoc solid-phase peptide synthesis (SPPS; Fmoc = 9-fluorenylmethoxycarbonyl). Despite several attempts using optimized protocols, we were unable to produce even trace amounts of the target molecule. Detailed MALDI analysis indicated complete termination of chain extension around residue Lys31.

To circumvent these problems, we turned to *tert*-butoxy-carbonyl (Boc) chemistry and employed a peptide-fragment ligation approach by using the native chemical ligation developed by Kent et al. (Scheme 1).^[5] This approach has been instrumental in enabling access to unrelated but similarly complex venom-derived disulfide-rich molecules.^[6] The synthesis strategy for Ma-2 employed three segments with Cys19 and Cys37 serving as ligation sites. Temporary protection of Cys19 was realized by substituting this residue with 1,3-thiazolidine-4-carboxylic acid.^[7] Peptide thioesters corresponding to Ma-2[1–18] and Ma-2[19–36] were assembled by optimized Boc SPPS, whereas Ma-2[37–57] was produced by using Fmoc chemistry.^[8] All peptide segments were obtained in high yield and purity and were subsequently joined using native chemical ligation in a consecutive one-pot fashion as described previously (for experimental details, see the Supporting Information).^[6c,7,9] The full-length polypep-

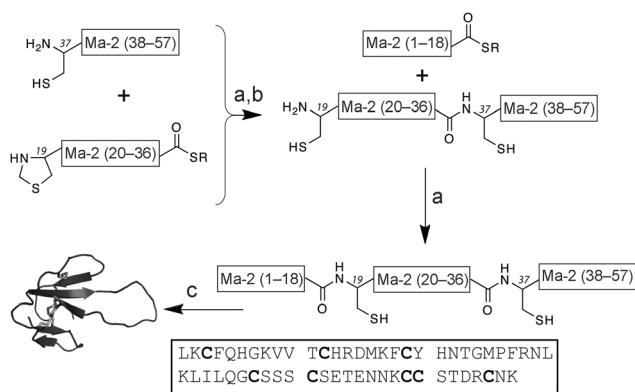
[*] Dr. C. I. Schroeder,^[+] Dr. L. D. Rash,^[+] X. Vila-Farrés, Prof. G. F. King, Prof. P. F. Alewood, Prof. D. J. Craik, Dr. T. Durek
Division of Chemistry and Structural Biology
Institute for Molecular Bioscience, The University of Queensland
Brisbane, Queensland (Australia)
E-mail: l.rash@imb.uq.edu.au
thomas.durek@gmail.com

Dr. K. J. Rosengren
School of Biomedical Sciences, The University of Queensland
(Australia)
Dr. M. Mobli
Centre for Advanced Imaging, The University of Queensland
(Australia)

[+] These authors contributed equally to this work.

[**] We gratefully acknowledge funding from the Australian National Health and Medical Research Council (NHMRC) (Grants 569927 to P.F.A. and 10123388 to L.D.R., P.F.A., and G.F.K.) and The University of Queensland. M.M. is supported by an Australian Research Council Future Fellowship, and G.F.K., K.J.R., and D.J.C. by NHMRC Fellowships. ASIC = acid-sensing ion channel.

Supporting information for this article is available on the WWW under <http://dx.doi.org/10.1002/anie.201308898>.



Scheme 1. Synthesis of Ma-2 by native chemical ligation of three peptide segments. a) native chemical ligation: GdmHCl (6 M), sodium phosphate (0.2 M), 4-mercaptophenylacetic acid (50 mM), tris(2-carboxyethyl)phosphine HCl (50 mM), pH 7.0; b) Thz→Cys conversion: methoxyamine HCl (0.3 M), pH 4.0; c) folding and disulfide formation: Tris (100 mM), GdmHCl (500 mM), GSH (8 mM), GSSG (1 mM), pH 8.0. Tris = tris(hydroxymethyl)aminomethane, GdmHCl = guanidine hydrochloride.

tide was obtained in good yield after HPLC purification (33%). Although peptides of this size are generally considered amenable to optimized stepwise SPPS,^[10] our experience suggests that fragment-based assembly may deliver superior results.

In vitro folding of the polypeptide chain and concomitant formation of the four disulfide bridges required optimization. Because of the large number of potential disulfide isomers (105), optimization was guided by HPLC analysis and activity testing of isolated fractions on rat (r) ASIC1a (see below). Folding was most efficient in Tris (100 mM), guanidine HCl (500 mM), pH 8.0 containing a redox system of reduced glutathione (GSH; 8 mM) and oxidized glutathione (GSSG; 1 mM). Under these conditions, the reaction reached equilibrium in 24 h and the correctly folded Ma-2 was isolated in high purity and acceptable yield after HPLC purification (11%). The activity of the synthetic material was assessed using two-electrode voltage-clamp electrophysiology on *Xenopus laevis* oocytes heterologously expressing homomeric rASIC1a and rASIC1b (Figure 1). The synthetic Ma-2 caused a concentration-dependent inhibition with an IC_{50} of (21 ± 6) nM for rASIC1a and (103 ± 13) nM for rASIC1b ($n = 5$). Both values

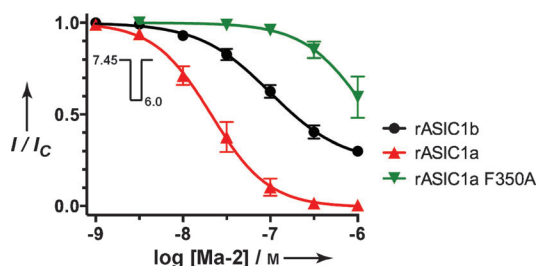


Figure 1. Functional characterization of synthetic Ma-2. Concentration-response curves for inhibition by synthetic Ma-2 of rASIC1a, rASIC1b, or an F350 A mutant of rASIC1a (all $n = 5$). I/I_c : test current/control current. The inset shows the pH-jump protocol used for channel activation.

are slightly lower (indicating higher potency) than the values reported for native Ma-2 isolated from snake venom (rASIC1a: 55 nM; rASIC1b: 192 nM),^[2a] thus underscoring the high quality of the synthetic material.

The 3D structure of the synthetic Ma-2 was determined by using homonuclear 2D NMR spectroscopy (see the Supporting Information). The solution structure of Ma-2 was calculated from 1003 interproton-distance and dihedral-angle restraints by using CYANA 3.0^[11] and refined by using CNS.^[12] Analysis of the secondary H_α chemical shifts compared to those found in random-coil peptides revealed several stretches of positive chemical shifts indicative of β -sheet formation (Supporting Information, SI Figure 3).^[13] Several residues, most notably Gly36, Arg54, and Arg57, experienced unusually large chemical shift differences most likely as a result of aromatic ring current effects owing to proximity to Tyr20 and Phe4 (SI Figure 3). Statistical analysis of the inferred disulfide-bond connectivity in the resultant structure was performed using PADLOC^[14] and was in agreement with the disulfide pattern Cys3–Cys19, Cys12–Cys37, Cys41–Cys49, and Cys50–Cys55.

An ensemble of the 20 lowest-energy structures of Ma-2 is shown in Figure 2a. Overall, the structure is well-defined and has a fold reminiscent of TFTs (SI Figure 4). The core of the molecule is stabilized by four disulfide bridges with the same

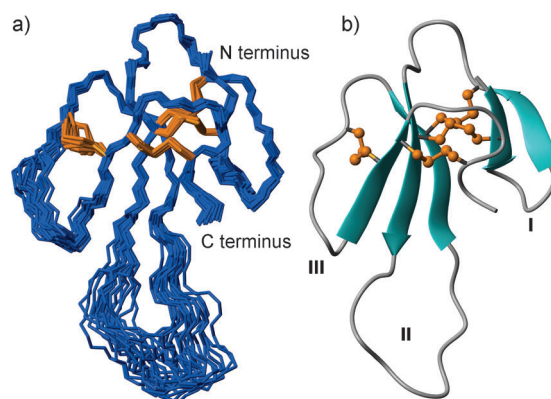


Figure 2. Structure of Ma-2. a) Ensemble of the 20 lowest-energy Ma-2 structures (PDB ID: 2MFA) superimposed over the backbone of the well-ordered sections composed of residues 1–22, 34–41, and 47–57. The N and the C termini are labeled and the four disulfide bonds are shown in orange. b) Ribbon representation of the lowest energy Ma-2 structure showing three fingers protruding from a disulfide-stabilized core. Note the two β -sheets; the antiparallel triple-stranded β -sheet includes fingers II and III while the antiparallel double-stranded β -sheet encompasses finger I.

connectivity as in other short-chain neurotoxins. Hydrogen-deuterium exchange TOCSY experiments indicated several slow-exchanging amide protons. In particular, the backbone amide protons of residues 10, 18, 20, and 52 were still detectable after 21 h, a result indicative of strong hydrogen bonding in the core of the molecule. Three loops protrude from this core (Figure 2b). The first (I; residues 4–11) and the third (III; residues 42–48) “fingers” are structurally well defined, although they are shorter than in other TFTs

(SI Figure 4). By contrast, the longer middle finger (II; residues 20–36) is disordered from Thr23 to Ile33, a result in agreement with TALOS-N predictions that this section is flexible.^[15] An extensive hydrogen-bonding network between fingers II and III gives rise to a three-pleated antiparallel β -sheet. Finger I forms a separate antiparallel β -sheet that is structurally constrained by the disulfides Cys3–Cys19 and Cys12–Cys37. This arrangement of secondary structural elements is characteristic for short-chain TFTs (SI Figure 4). Despite the similar core, the structure of Ma-2 stands out among TFTs as a result of its short first and third fingers and elongated middle finger.

The peptide surface contains several clusters of basic or acidic residues (Figure 3a, upper panel): 1) a large, positively charged cluster located in the first finger and the core domain; 2) Glu43 and Glu45 in the third finger; and 3) Arg28 and Lys31 located at the tip of the middle finger. The latter is

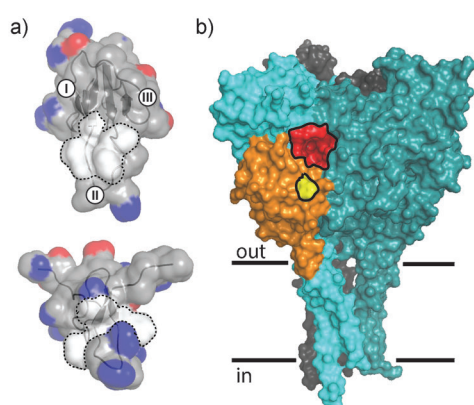


Figure 3. Structural characterization of synthetic Ma-2. a) Surface charge distribution of Ma-2 (upper panel) and Pctx1 (PDB ID: 2KNI, lower panel).^[21] The hydrophobic patch is colored white and the Ma-2 fingers are labeled I–III. b) Structure of chicken ASIC1 (PDB ID: 4FZO).^[17a] The three subunits that form the functional channel are shown in cyan, turquoise, and gray and the locations of the acidic pocket (red), Phe350 (yellow), and the thumb region (orange) are indicated.

adjacent to a hydrophobic patch formed by Met25, Phe27, Leu30, Leu32, and Leu34. This arrangement is reminiscent of psalmotoxin 1 (Pctx1), a potent modulator of ASIC1 isolated from tarantula venom (Figure 3a, lower panel).^[16] Pctx1 binds to the acidic pocket at the interface between ASIC1 subunits (Figure 3b) that serves as a putative proton-sensing site.^[17] In doing so, Pctx1 alters the proton sensitivity of the channel and stabilizes the desensitized state. Interestingly, mambalgins have been shown to decrease ASIC sensitivity to protons, thus suggesting that they might also act as gating modifiers and directly or indirectly interfere with the proton-sensing mechanism.^[2a]

Based on the structural and potential mechanistic similarities between Pctx1 and Ma-2, we hypothesized that these toxins might target the same site on ASIC1.

To test this hypothesis, we generated a variant of rASIC1a carrying an F350A mutation. This residue, which is highly conserved in ASIC1, is located on α -helix 5 (the “thumb

region”), just outside the acidic pocket (Figure 3b). An F350L mutation was previously shown to essentially abolish the action of Pctx1 on human ASIC1a.^[18] The F350A-mutant channel functioned similarly to wild-type rASIC1a albeit with an acidic shift in the pH sensitivity of steady-state desensitization and activation ($\Delta\text{pH}_{0.5} = -0.17$ and -0.37 , respectively, see SI Figure 5; $\text{pH}_{0.5}$ = the pH value that causes half-maximal activation). This is not surprising given that Phe350 lies adjacent to the proton-sensing residue Asp349, and the F350L mutation in hASIC1a resulted in the $\text{pH}_{0.5}$ of activation undergoing a similar acidic shift of approximately 0.4 pH units.^[18] The mutant channel was dramatically less sensitive to Ma-2 than wild-type rASIC1a ($\text{IC}_{50} > 1 \mu\text{M}$, Figure 1). This more than 50-fold drop in toxin efficacy indicates that Phe350 plays a key role in sensitizing ASIC1a channels towards Ma-2 as it does in sensitizing them towards Pctx1.^[18]

Pctx1 is an equipotent inhibitor of ASIC1a homomers and ASIC1a/2b heteromers^[18] and potentiates ASIC1b homomers,^[19] whereas the mambalgins inhibit both ASIC1a and ASIC1b homomers and ASIC1a heteromers (with either 1b, 2a or 2b).^[2a] It thus seems that both peptides can interact, with similar relative efficacy, with the same range of ASIC subtypes.^[19] In light of their similar subtype selectivities and the fact that both toxins require F350 for functional interaction with ASIC1, it seems likely that they have similar binding sites, albeit with varied functional consequences (Pctx1 can potentiate ASICs,^[19] whereas mambalgins have to date only been reported to cause inhibition).

In summary, we demonstrated efficient chemical synthesis of the analgesic venom peptide Ma-2. We anticipate not only that our synthetic approach will enable detailed structure–activity studies of Ma-2 but that it will also be applicable to other family members as a result of the high degree of sequence conservation within the mambalgin family. We provide the first experimental proof that mambalgins adopt a TFT fold. The mambalgins therefore represent another example of the evolutionary divergence of the TFT fold in order to functionally diversify the toxin repertoire of venomous snakes.^[20] Finally, our functional data suggest that the mambalgins bind in close proximity to the acidic pocket of ASIC channels in a manner very similar to that of Pctx1, most likely by insertion of one of their protruding “fingers”.

Received: October 12, 2013

Published online: December 9, 2013

Keywords: ion channels · native chemical ligation · NMR spectroscopy · peptides · solid-phase synthesis

- [1] S. Dutertre, R. J. Lewis, *J. Biol. Chem.* **2010**, *285*, 13315–13320.
- [2] a) S. Diochot et al., *Nature* **2012**, *490*, 552–555; b) D. J. Craik, C. I. Schroeder, *Angew. Chem.* **2013**, *125*, 3149–3151; *Angew. Chem. Int. Ed.* **2013**, *52*, 3071–3073.
- [3] E. Deval, X. Gasull, J. Noel, M. Salinas, A. Baron, S. Diochot, E. Lingueglia, *Pharmacol. Ther.* **2010**, *128*, 549–558.
- [4] Y. N. Utkin, *Toxicon* **2013**, *62*, 50–55.
- [5] P. E. Dawson, T. W. Muir, I. Clark-Lewis, S. B. Kent, *Science* **1994**, *266*, 776–779.

- [6] a) J. E. Jensen, T. Durek, P. F. Alewood, D. J. Adams, G. F. King, L. D. Rash, *Toxicon* **2009**, *54*, 56–61; b) R. A. Morales et al., *ChemBioChem* **2010**, *11*, 1882–1888; c) T. Durek, I. Vetter, C. I. A. Wang, L. Motin, O. Knapp, D. J. Adams, R. J. Lewis, P. F. Alewood, *ACS Chem. Biol.* **2013**, *8*, 1215–1222.
- [7] D. Bang, S. B. Kent, *Angew. Chem.* **2004**, *116*, 2588–2592; *Angew. Chem. Int. Ed.* **2004**, *43*, 2534–2538.
- [8] M. Schnölzer, P. Alewood, A. Jones, D. Alewood, S. B. Kent, *Int. J. Pept. Protein Res.* **1992**, *40*, 180–193.
- [9] A. Ghassemian, C. I. A. Wang, M. K. Yau, R. C. Reid, R. J. Lewis, D. P. Fairlie, P. F. Alewood, T. Durek, *Chem. Commun.* **2013**, *49*, 2356–2358.
- [10] S. B. Kent, *Annu. Rev. Biochem.* **1988**, *57*, 957–989.
- [11] P. Güntert, C. Mumenthaler, K. Wüthrich, *J. Mol. Biol.* **1997**, *273*, 283–298.
- [12] A. T. Brünger et al., *Acta Crystallogr. Sect. D* **1998**, *54*, 905–921.
- [13] D. S. Wishart, C. G. Bigam, A. Holm, R. S. Hodges, B. D. Sykes, *J. Biomol. NMR* **1995**, *5*, 67–81.
- [14] L. Poppe, J. O. Hui, J. Ligutti, J. K. Murray, P. D. Schnier, *Anal. Chem.* **2012**, *84*, 262–266.
- [15] Y. Shen, F. Delaglio, G. Cornilescu, A. Bax, *J. Biomol. NMR* **2009**, *44*, 213–223.
- [16] P. Escoubas, J. R. De Weille, A. Lecoq, S. Diochot, R. Waldmann, G. Champigny, D. Moinier, A. Menez, M. Lazdunski, *J. Biol. Chem.* **2000**, *275*, 25116–25121.
- [17] a) I. Bacongus, E. Gouaux, *Nature* **2012**, *489*, 400–405; b) M. Salinas, L. D. Rash, A. Baron, G. Lambeau, P. Escoubas, M. Lazdunski, *J. Physiol.* **2006**, *570*, 339–354; c) R. J. P. Dawson et al., *Nat. Commun.* **2012**, *3*, 936.
- [18] T. Sherwood, R. Franke, S. Conneely, J. Joyner, P. Arumugan, C. Askwith, *J. Biol. Chem.* **2009**, *284*, 27899–27907.
- [19] A. Baron, S. Diochot, M. Salinas, E. Deval, J. Noel, E. Lingueglia, *Toxicon* **2013**, *75*, 187–204.
- [20] R. M. Kini, R. Doley, *Toxicon* **2010**, *56*, 855–867.
- [21] N. J. Saez et al., *Mol. Pharm.* **2011**, *80*, 796–808.